Clinical and Experimental Health Sciences

Investigation of Anti-Cancer Efficiency of DZNep and Stauprimide Combination in Breast Cancer

Çağlar Çelebi[1], Tuğçe Balcı Okcanoğlu[2], Çağla Kayabaşı[3], Besra Özmen Yelken[4], Aycan Aşık[5], Röya Gasımlı[1], Eda Tayfur[1], Cumhur Gündüz[1]

[1] Ege University, Faculty of Medicine, Department of Medical Biology, Izmir, Türkiye.
[2] University of Kyrenia, Faculty of Medicine, Medical Biology Department, Karakum Kyrenia TRNC.
[3] Balıkkesir University, Faculty of Medicine, Department of Medical Biology, Balıkesir, Türkiye.
[4] Bakircay University, Faculty of Medicine, Department of Medical Biology, Izmir, Türkiye.
[5] Muğla Sıtkı Koçman University, Faculty of Medicine, Department of Medical Biology, Muğla, Türkiye.

Correspondence Author: Tuğçe Balci Okcanoğlu
E-mail: tbalcii@gmail.com

Received: April 09, 2025 **Accepted:** August 29, 2025

ABSTRACT

Objective: Breast cancer represents a significant clinical challenge due to tumor heterogeneity and the presence of therapy-resistant cancer stem cells (CSCs). The combination of epigenetic modulators and differentiation-inducing agents has emerged as a promising therapeutic strategy. In this study, we aimed to evaluate the anticancer effects of combining the methyltransferase inhibitor 3-Deazaneplanocin A (DZNep) and the MYC transcription inhibitor Stauprimide on breast cancer cell lines and breast cancer stem cells (BCSCs).

Methods: Cytotoxicity was determined by real-time cell analysis (RTCA) to calculate IC_{50} values and evaluate the synergistic potential of the combination using isobologram analyses. Apoptosis induction and cell cycle distribution were assessed via flow cytometry using Annexin V-FITC/PI staining and DNA content analysis, respectively. Cell migration was evaluated using wound-healing assays. Additionally, quantitative RT-PCR was performed to analyze expression changes in key apoptosis – and cell cycle-related genes following treatment.

Results: The combination of DZNep and Stauprimide (1:1 ratio) demonstrated significant synergistic cytotoxicity in MCF-7 (luminal A) and MDA-MB-231 (triple-negative) breast cancer cells, substantially reducing effective doses of both agents (combination index values of 0.671 and 0.134, respectively). Treatment markedly induced apoptosis, triggered cell cycle arrest predominantly at G2/M and G0/G1 phases, increased polyploidy, and significantly inhibited migration. Notably, the combination selectively induced apoptosis and modulated gene expression (e.g., TP53 and p27 upregulation) in BCSCs, while exhibiting minimal toxicity towards the normal mammary epithelial cell line, MCF-10A. The combination of DZNep and Stauprimide exerts potent anticancer effects by selectively inducing apoptosis, cell cycle arrest, and suppressing migration in breast cancer cells, including CSC populations.

Conclusion: These findings suggest translational potential for preventing recurrence and metastasis, positioning this therapeutic strategy as a promising candidate for further validation in preclinical and clinical studies.

Keywords: Breast Cancer, DZNep, Stauprimide, Drug Combination, Cancer stem cells

1. INTRODUCTION

Breast cancer remains the most prevalent malignancy among women worldwide, representing a significant global health challenge across both developed and developing countries. According to the GLOBOCAN 2020 report, breast cancer accounted for approximately 2.3 million new cases and 685,000 deaths, representing 15.5% of all cancer-related mortalities in women [1]. In response to this growing burden, the World Health Organization (WHO) launched the Global Breast Cancer Initiative in 2021, emphasizing early diagnosis, effective treatment strategies, and integrated patient management to improve outcomes [2]. Breast cancer is a heterogeneous disease and is primarily classified into two major categories based on estrogen receptor (ER) status: ER-positive and ER-negative tumors. ER-positive tumors exhibit activation of estrogen-responsive genes and luminal epithelial-specific transcripts and are further subtyped into luminal A and luminal B based on gene expression signatures and proliferation indices [3,4]. ER-negative tumors, including HER2-positive and basal-like subtypes, are typically more aggressive and often exhibit enhanced expression of genes within the HER2 amplicon—such as growth factor receptor-bound protein 7 (*GRB7*)—as well as hyperactivation of oncogenic pathways like NF-κB [3]. Among the key contributors to breast cancer heterogeneity and therapeutic resistance are breast cancer stem cells (BCSCs), a

How to cite this article: Çelebi Ç, Okcanoğlu TB, Kayabaşı Ç, Yelken BÖ, Aşık A, Gasımlı R, Tayfur E, Gündüz C. Investigation of Anti-Cancer Efficiency of DZNep and Stauprimide Combination in Breast Cancer. Clin Exp Health Sci 2025; 15: 724-734. https://doi.org/10.33808/clinexphealthsci.1672477

subpopulation characterized by $CD44^{high}/CD24^{low}$ expression and elevated *ALDH1* activity [5,6]. These cells possess the capacity for asymmetric division, enabling both self-renewal and differentiation into various tumor cell types, which in turn contributes to tumor recurrence, metastasis, and resistance to standard therapies [7–9].

Early arising of intrinsic or acquired chemotherapy (CT) resistance is common and represents the main hurdle for successful TNBC treatment [10]. Notably, while conventional therapies can effectively eliminate bulk tumor cells, BCSCs often persist, evading treatment through alternative signaling cascades [11] such as Notch, Wnt, and Hedgehog, as well as through epigenetic plasticity [12–14]. Consequently, current therapeutic strategies are increasingly focusing on targeting epigenetic regulators that maintain stemness in BCSCs to enhance long-term treatment efficacy [15,16]. Epigenetic dysregulation plays a pivotal role in breast cancer pathogenesis, with particular emphasis on enhancer of zeste homolog 2 (EZH2), a histone methyltransferase that catalyzes trimethylation of histone H3 on lysine 27 (H3K27me3). EZH2 is frequently overexpressed in various cancers [17], including breast cancer, where its elevated expression correlates with poor prognosis and aggressive clinical behavior [18,19]. Importantly, EZH2 acts by repressing tumor suppressor genes, and its druggability has made it an attractive therapeutic target. 3-Deazaneplanosin A (DZNep), an indirect inhibitor of EZH2, has been shown to reduce H3K27me3 levels, induce apoptosis, arrest the cell cycle, and promote differentiation in multiple cancer models [20]. Concurrently, the MYC oncogene, which is dysregulated in over 70% of human cancers and in up to 30% of breast cancers—especially in TNBC and HER2-enriched subtypes—has been implicated in driving uncontrolled proliferation, metabolic reprogramming, and therapy resistance [21]. MYC also plays a central role in regulating cell cycle progression, apoptosis suppression, angiogenesis, and immune evasion [22]. Stauprimide is a small molecule inhibitor of MYC transcription [23–24] and has demonstrated potential in promoting differentiation and inducing cell cycle arrest in various cancer models, including pluripotent stem cells [25,26]. However, its role in breast cancer, particularly in targeting BCSCs, remains largely unexplored.

Given that EZH2 and MYC are part of a regulatory oncogenic axis—with reciprocal transcriptional regulation and cooperative roles in tumor progression—their simultaneous inhibition may offer a mechanistically sound and potentially synergistic therapeutic strategy [27]. DZNep and Stauprimide, through their respective epigenetic and transcriptional mechanisms, may disrupt critical feedback loops sustaining tumor growth and BCSC maintenance, thus enhancing therapeutic efficacy. In this study, we aimed to evaluate the individual and combinatory anti-cancer effects of DZNep and Stauprimide on various breast cell models, including the normal mammary epithelial cell line (MCF-10A), luminal A breast cancer cell line (MCF-7), triple-negative breast cancer cell line (MDA-MB-231), and an enriched population of breast cancer stem cells (BCSCs). Specifically, we investigated their impact on cytotoxicity, apoptosis, cell cycle progression, migration, and gene expression profiles. A major focus was to determine whether the combination selectively targets BCSCs while sparing normal epithelial cells, thereby offering a potentially novel and selective therapeutic approach for breast cancer.

2. METHODS

2.1. Chemicals and Cell Lines

3-Deazaneplanosin A (DZNep; Cat. No: S7120, Selleckchem, USA) and Stauprimide (Cat. No: S2951, Sigma-Aldrich, USA) were dissolved in 100% dimethyl sulfoxide (DMSO) to prepare 10 mM stock solutions and stored at −20 °C. Human breast cancer cell lines MDA-MB-231 (triple-negative), MCF-7 (luminal A), MCF-10A (non-tumorigenic epithelial control), and breast cancer stem cells (BCSCs) were obtained from the American Type Culture Collection (ATCC, USA). Cells were cultured under humidified conditions at 37 °C in 5% CO_2. Cell lines were maintained in ATCC-recommended media supplemented with appropriate growth factors and sera. Specifically, MCF-10A was cultured in DMEM/F12 supplemented with EGF, hydrocortisone, insulin, cholera toxin, and 5% horse serum.

2.2. Cytotoxicity and Combination Analysis

The cytotoxic effects of DZNep and Stauprimide, individually and in combination, were evaluated using the xCELLigence Real-Time Cell Analysis System (RTCA-SP, Roche Applied Science, Germany). Cells were seeded in 96-well E-plates at the following densities: MCF-7, 1.3×10^4 cells/mL; MDA-MB-231, 1.5×10^4 cells/mL; MCF-10A, 2.2×10^4 cells/mL; and BCSCs, 8×10^3 cells/mL. The Cell Index (CI) was monitored at 24, 48, and 72 hours post-treatment. Half-maximal inhibitory concentrations (IC_{50}) and effective dose values (ED_{50}) were calculated using dose–response curves. Drug interactions were assessed using a fixed-ratio (1:1) combination design. Combination Index (CI) and Dose Reduction Index (DRI) values were determined via isobologram analysis using Calcusyn software (v2.0, Biosoft, UK). CI values were interpreted as follows: CI < 1 indicates synergism, CI = 1 additive effect, and CI > 1 antagonism [28].

2.3. Apoptosis Analysis

Apoptosis was assessed at 72 hours using Annexin V/PI dual staining and flow cytometry. Cells (2×10^4/well) were seeded into 6-well plates and treated with IC_{50} or ED_{50} doses of DZNep and/or Stauprimide. Apoptotic cells were stained using the FITC Annexin V Apoptosis Detection Kit (BD Pharmingen, USA), and analyzed with the BD Accuri C6 flow cytometer. Data were interpreted using BD CFlow v1.0 software. Apoptotic cells were defined as Annexin V^+/PI^- (early apoptosis) and Annexin V^+/PI^+ (late apoptosis). Fold-changes were calculated relative to untreated controls.

2.4. Cell Cycle Analysis

To assess cell cycle distribution, cells treated for 72 hours were fixed in 70% ethanol and analyzed using the BD Cycletest Plus DNA Reagent Kit (BD Biosciences, USA) according to the manufacturer's protocol. DNA content was measured by flow cytometry, and the percentage of cells in G0/G1, S, and G2/M phases was calculated. Polyploidy (≥4n DNA content) was

quantified as an indicator of mitotic aberrations. Data were analyzed using BD CFlow v1.0 software.

2.5. Cell Migration (Wound Healing) Assay

The scratch assay was used to assess cell migration. Cells (2×10^4/well) were seeded in 6-well plates and grown to 90% confluency. A uniform scratch was created using a sterile 200 µL pipette tip. IC_{50} and ED_{50} doses of the compounds were added immediately post-scratch. Images were captured at 0, 24, 48, and 72 hours using an Olympus IX73 inverted microscope equipped with a DP72 digital camera. Wound closure was quantified using ImageJ software and calculated as the percentage change in wound area compared to baseline.

2.6. Gene Expression Analysis

Total RNA was isolated from cells (2×10^4/well) at 72 hours post-treatment using the RNeasy Mini Kit (Qiagen, Germany), and purity was confirmed via NanoDrop 2000c spectrophotometry (Thermo Scientific, USA). Total RNA samples with A260/280 and A230/260 ratios ≥2.0 were used. Complementary DNA (cDNA) synthesis was performed with the iScript cDNA Synthesis Kit (Bio-Rad, USA). Quantitative RT-PCR was conducted using the LightCycler 480 II system (Roche, Switzerland) to evaluate the expression of genes related to apoptosis (*BAX, BCL2*), cell cycle regulation (*TP53, RB1*, p16, p21, p27), and oncogenic signaling (*MYC*). In the qRT-PCR analysis, SsoAdvanced Universal SYBR Green Supermix and primers were used. *GAPDH* and *ACTB* were used as internal reference genes. Primer designs *BAX F (5'→3'): GCTGGACATTGGACTTCCTC R (5'→3'):CTCAGCCCATCTTCTTCCAG / BCL2 F (5'→3'): AGATGGGAACACTGGTGGAG R (5'→3'):CTTCCCCAAAAGAAATGCAA / TP53 F (5'→3'): GGCCCACTTCACCGTACTAA R (5'→3'):GTGGTTTCAAGGCCAGATGT / RB1 F (5'→3'): CAAACTTGGAGTTCGCTTGT R (5'→3'): TTCAGAATCCATGGGAAAGA / CDKN2A (p16^INK4a) F (5'→3'): TCCCCCACTACCGTAAATGT R (5'→3'): TCATGAAGTCGACAGCTTCC / CDKN1A (p21^Cip1) F (5'→3'): AAACTTTGGAGTCCCCTCAC R (5'→3'): AAAGGCTCAACACTGAGACG / CDKN1B (p27^Kip1) F (5'→3'):TCAAACGTGCGAGTGTCTAA R (5'→3'): CCACTCGTACTTGCCCTCTA / MYC F (5'→3'): CGACGAGACCTTCATCAAAA R (5'→3'): TGCTGTCGTTGAGAGGGTAG / GAPDH F (5'→3'):GAGTCAACGGATTTGGTCGT R (5'→3'): TTGATTTTGGAGGGATCTCG / ACTB (ß-actin) F (5'→3'): GAGCGCGGCTACAGCTT R (5'→3'): TCCTTAATGTCACGCACGATTT.* Relative gene expression levels were calculated using the $2^{-\Delta\Delta Ct}$ method. Statistical analyses (*Students' t*-test) of gene expression data were performed via the Qiagen GeneGlobe Data Analysis Center [29].

2.7. Statistical Analysis

All experiments were conducted in at least three independent biological replicates. Quantitative results were presented as mean ± standard deviation (SD). One-way analysis of variance (ANOVA) followed by *Tukey's post hoc* test was used to compare multiple groups. A p-value of <.05 was considered statistically significant. All statistical analyses were performed using GraphPad Prism v5.0 (GraphPad Software, USA).

3. RESULTS

3.1. Cytotoxicity Analysis

The cytotoxic effects of DZNep and Stauprimide on various breast cell lines were assessed through IC_{50} values calculated from dose-response curves at 72 hours post-treatment. DZNep exhibited IC_{50} values of 182.75 µM, 115.00 µM, 105.80 µM, and 108.61 µM in MDA-MB-231, MCF-7, BCSC, and MCF-10A cells, respectively (Figure 1). In contrast, IC_{50} values for Stauprimide were notably lower in the triple-negative MDA-MB-231 cell line (2.47 µM), while higher values were observed in MCF-7 (115.00 µM), BCSC (97.30 µM), and normal mammary epithelial MCF-10A cells (19.90 µM). These results highlight the differential sensitivity of cancer versus normal cells, indicating a potentially favorable therapeutic window, especially for Stauprimide.

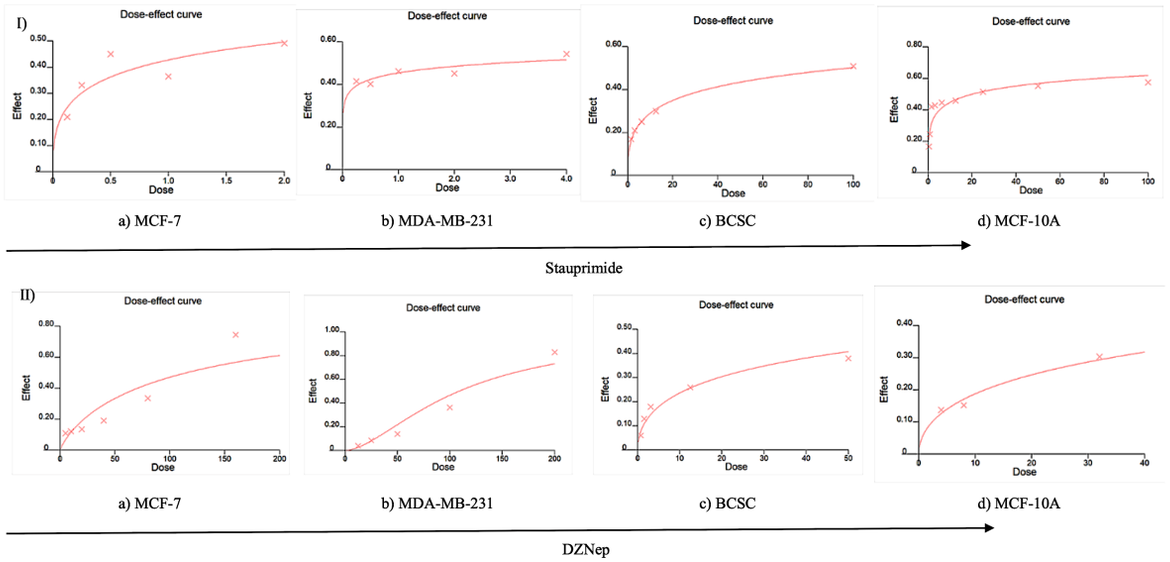

Figure 1. *Dose–response curves for (I) Stauprimide and (II) DZNep in (a) MCF-7, (b) MDA-MB-231, (c) breast cancer stem cells (BCSC), and (d) MCF-10A cell lines. IC_{50} values were determined based on real-time cell impedance analysis relative to untreated control groups.*

3.2. Combination Efficacy: Isobologram, Combination Index (CI), and Dose Reduction Index (DRI)

The combined effect of Stauprimide and DZNep at an equimolar ratio (1:1) was evaluated using isobologram analyses. In the MCF-7 cell line, the calculated CI at the ED_{50} concentration was 0.671, indicative of a synergistic interaction (Figure 2, Table 1). Correspondingly, the dose reduction index (DRI) for DZNep was substantial (83.98-fold), underscoring the enhanced efficacy and reduced therapeutic dosage achievable through combination therapy. The combination showed even stronger synergy in MDA-MB-231 cells (CI = 0.134) with a remarkable dose reduction for DZNep (DRI = 502.33-fold). Conversely, an additive interaction (CI = 1.019) was observed in the BCSC cell line, though the dose reductions remained considerable for both drugs (DRI > 2). The comparatively higher doses required for cytotoxic effects in normal MCF-10A cells suggest a favorable selectivity profile, reinforcing the combination's potential for targeted cancer therapy with minimal toxicity to normal tissues.

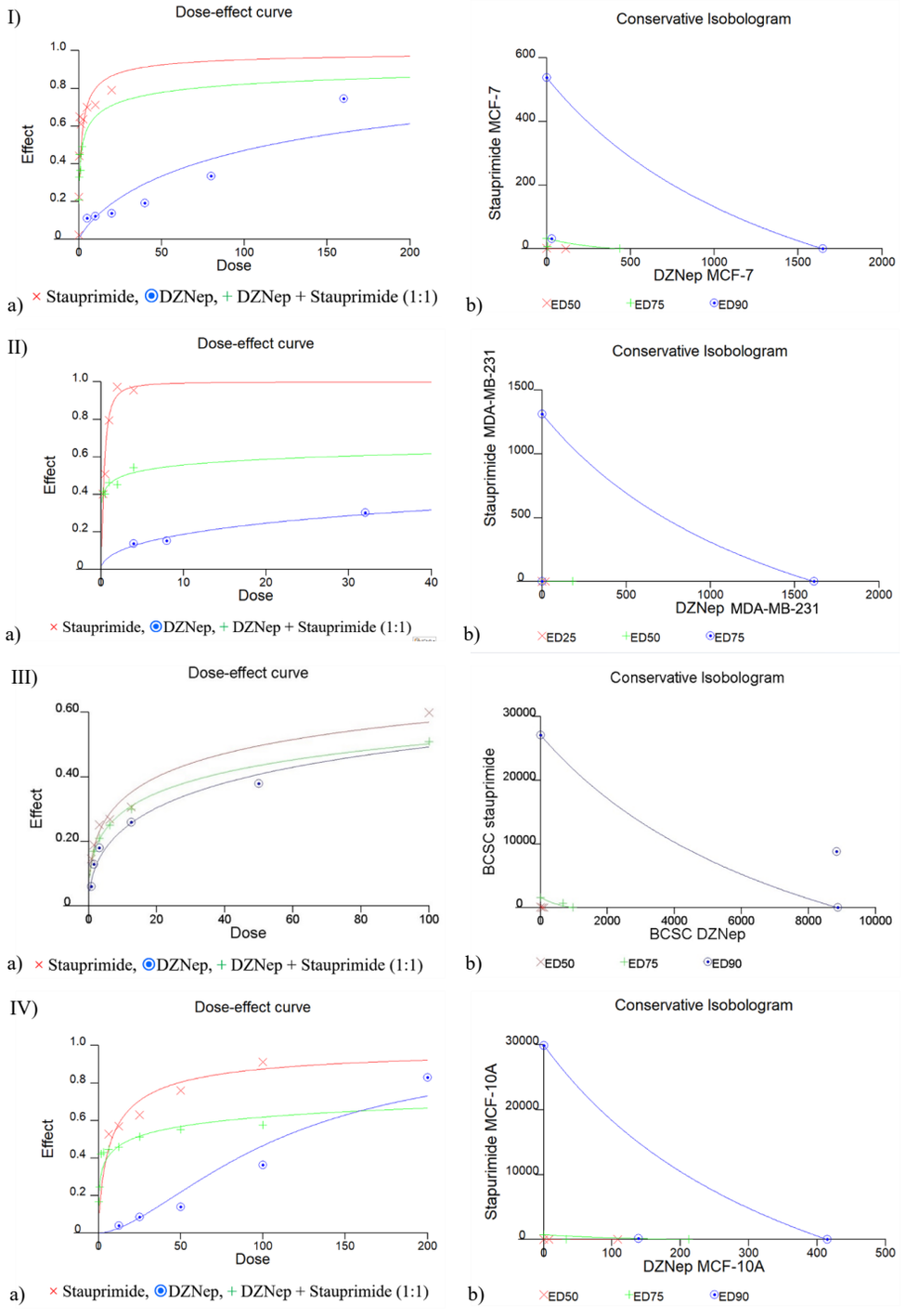

Figure 2. *(a) Dose–response curves and (b) corresponding conservative isobologram plots illustrating the effects of Stauprimide and DZNep combination (1:1 molar ratio) on (I) MCF-7, (II) MDA-MB-231, (III) BCSC, and (IV) MCF-10A cell lines. Calculated ED_{50} values for the combination treatment were 1.36 µM (MCF-7), 0.36 µM (MDA-MB-231), 7.90 µM (BCSC), and 51.66 µM (MCF-10A), respectively. All comparisons were made against vehicle-treated control cells.*

Table 1. *Synergistic effects of Stauprimide and DZNep combination on breast cancer cell lines.*

Cell lines	ED_{50} (μM)		CI	DRI	
	Stau	DZN		Stau	DZN
MCF-7	1.36	1.36	0.671	1.517	83.983
MDA-MB-231	0.36	0.36	0.134	7.556	502.327
MCF-10A	7.90	7.90	0.470	2.518	13.749
BCSC	51.66	51.66	1.019	1.883	2.048

Cells were treated with a combination of Stauprimide and DZNep at a fixed ratio of 1:1 for 72 hours. Inhibitory concentrations (IC_{50} and ED_{50}) and combinational effects were calculated using CalcuSyn software based on real-time cell analysis (xCELLigence) data. Combination index (CI) values indicate interaction types: synergism (CI < 1), additive effect (CI = 1), and antagonism (CI > 1). Dose reduction index (DRI) values represent the fold-reduction in dose required to achieve 50% growth inhibition (fraction affected = 0.5) in combination relative to single-drug treatments. CI, combination index; DRI, dose reduction index; Stau, Stauprimide; DZN, DZNep.

3.3. Apoptosis Analysis

The induction of apoptosis following treatment was quantified by Annexin V-FITC/PI staining and flow cytometry. After 72 hours of exposure to IC_{50} and ED_{50} doses, apoptosis rates significantly increased compared to untreated controls. In MCF-7 cells, apoptosis reached 92.1% with Stauprimide (IC_{50}), 23.1% with DZNep (IC_{50}), and 79.1% with the combination treatment (ED_{50}), compared to 14.7% in controls. Similarly, in BCSCs, apoptotic cell rates were markedly elevated to 74.50% with Stauprimide, 5.4% with DZNep, and 66.3% with the combination, relative to 10.0% in untreated controls. Apoptosis rates in MDA-MB-231 cells were comparatively lower, reaching 14.1% with Stauprimide, 3.5% with DZNep, and 7.1% with combination treatment, compared to a control rate of 2.7%. Importantly, apoptosis in normal MCF-10A cells was less pronounced, highlighting a selective induction of apoptosis in cancer cells (Figure 3, Supplementary Figure 1; $p < .05$).

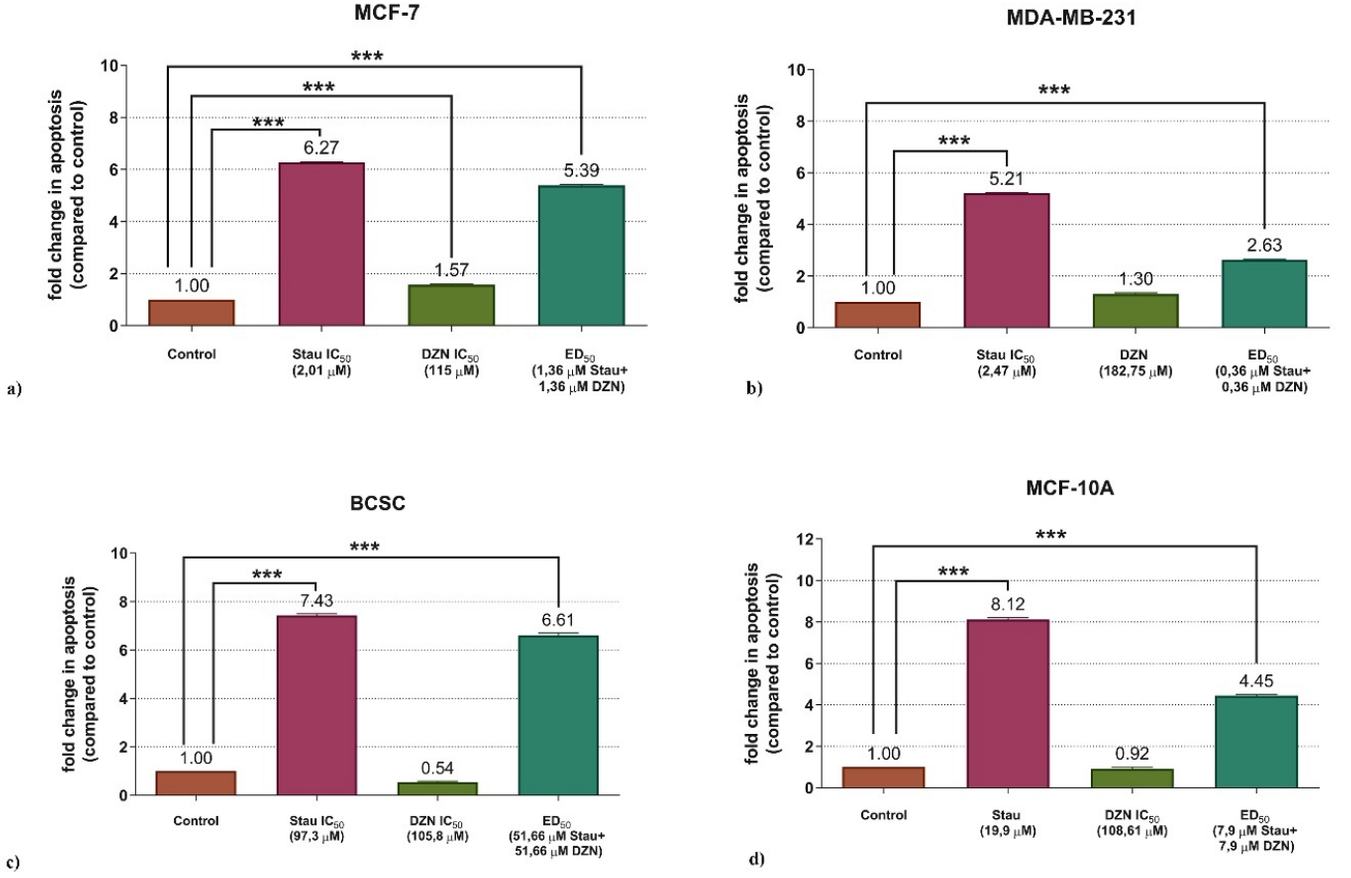

Figure 3. *Induction of apoptosis following single or combined treatment with Stauprimide and DZNep in (a) MCF-7, (b) MDA-MB-231, (c) BCSC, and (d) MCF-10A cells. Fold changes represent the proportion of early and late apoptotic cells as determined by Annexin V-FITC/PI staining and flow cytometry. Notably, the combination therapy significantly enhanced apoptosis, especially in MCF-7 and BCSC lines, even at lower doses than the individual treatments.*

3.4. Cell Cycle Analysis

Cell cycle phase distributions were analyzed to investigate the effects of treatments on cell cycle arrest and polyploidy formation. In MCF-7 cells, Stauprimide significantly induced G2/M arrest (63.8%) accompanied by notable polyploidy (14.1%), whereas DZNep primarily caused G0/G1 arrest (70.8%) with minimal polyploidy (1.0%). The combination treatment increased the proportion of cells in the G2/M phase to 42.7%, along with moderate polyploidy (5.8%). For MDA-MB-231 cells, Stauprimide increased G2/M phase arrest (41.4%) and polyploidy (28.8%), while DZNep led to modest G2/M arrest (35.9%) and polyploidy (21.3%). Interestingly, the combination treatment predominantly caused G0/G1 phase accumulation (40.8%) with polyploidy (17.6%). In the BCSC line, Stauprimide treatment resulted in G2/M accumulation (50.2%) and polyploidy (13.6%), whereas neither DZNep nor the combination significantly altered cell cycle distribution. Finally, in normal MCF-10A cells, Stauprimide induced moderate G2/M accumulation (29.3%) with minimal polyploidy (2.6%), and the combination treatment similarly caused a modest increase in G2/M phase cells (34.6%) with limited polyploidy (3.2%). These data collectively suggest that Stauprimide predominantly induces G2/M arrest and polyploidy, particularly in aggressive cancer cells, whereas DZNep preferentially affects the G0/G1 phase in specific cancer subtypes (Figure 4, Supplementary Figure 2).

3.5. Cell Migration (Wound Healing) Analysis

Cell migration assays revealed that treatment with Stauprimide, DZNep, or their combination significantly inhibited cell migration compared to untreated controls. After 72 hours, the remaining open wound area in MCF-7 cells increased markedly with Stauprimide (71.8%), DZNep (61.9%), and combination treatment (69.9%) relative to control conditions (36.1%). Similar inhibitory effects were observed in MDA-MB-231 cells, with the open wound area increased from 43.17% (untreated control) to 64.5% (Stauprimide) and 57.1% (combination). For BCSCs, the combination treatment notably increased the open area to 66.4% compared to 40.7% in untreated cells. Notably, normal MCF-10A cells exhibited complete wound closure under control conditions, whereas combination treatment markedly hindered wound closure, leaving 57.3% of the area open after 72 hours. Thus, these findings highlight the potential anti-metastatic capacity of the drug combination, with more pronounced effects observed in malignant cells (Figure 5, $p < .05$).

3.6. Gene Expression Analysis

Quantitative RT-PCR analysis was performed 72 hours post-treatment to evaluate changes in apoptosis – and cell cycle-related gene expression. In MCF-7 cells, treatment with Stauprimide and the combination significantly upregulated RB1 and p21 expression, whereas DZNep markedly increased *TP53* and *BAX* expression levels. In MDA-MB-231 cells, DZNep and combination treatments enhanced the expression of p27 and p16 genes. In BCSCs, combination treatment led to significant upregulation of *TP53* and p27. By contrast, in normal MCF-10A cells, gene expression changes were minimal and not significant. Gene expression data are summarized in Tables 2–5. Relative gene expression values, normalized against housekeeping genes and calculated via the $2^{-\Delta\Delta Ct}$ method, are detailed in supplementary data files along with relevant figures and statistical analyses (Supplementary File).

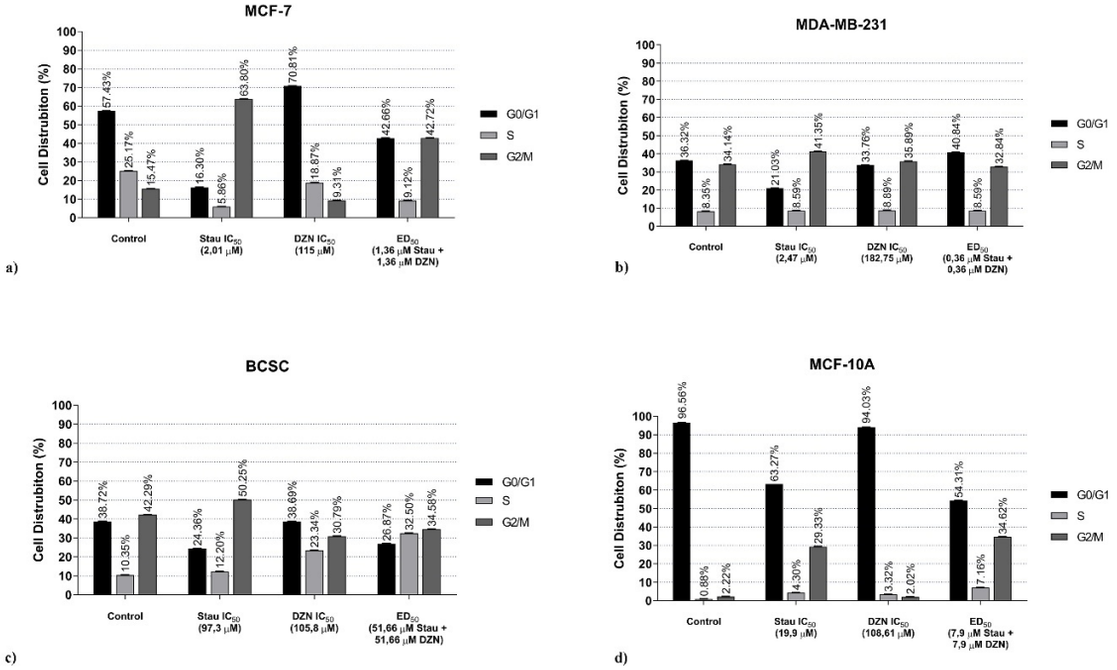

Figure 4. *Distribution of cell cycle phases following treatment with Stauprimide, DZNep, or their combination in (a) MCF-7, (b) MDA-MB-231, (c) BCSC, and (d) MCF-10A cell lines. Stauprimide predominantly induced G_2/M arrest in MCF-7 and BCSC cells, while DZNep induced G_0/G_1 arrest in MCF-7. In MDA-MB-231 cells, both agents promoted G_2/M arrest, whereas the combination resulted in G_0/G_1 phase accumulation. In MCF-10A cells, combination treatment led to a moderate G_2/M arrest.*

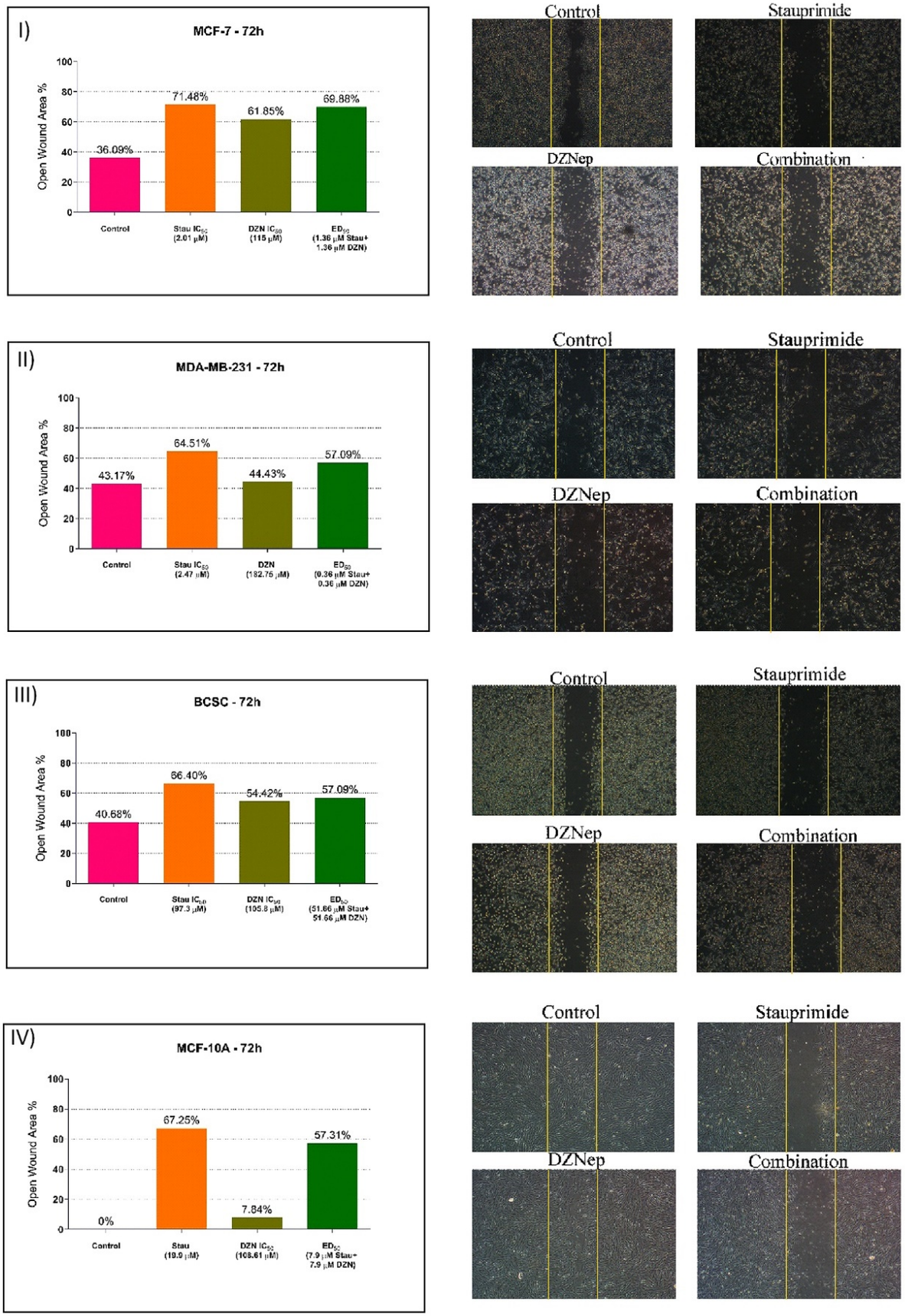

Figure 5. *Wound healing assay results showing the effects of Stauprimide, DZNep, and their combination on cell migration in (I) MCF-7, (II) MDA-MB-231, (III) BCSC, and (IV) MCF-10A cell lines. Relative wound closure percentages were quantified using ImageJ software and compared to untreated controls after 72 hours. Combination treatment markedly suppressed cellular migration, supporting its anti-metastatic potential.*

Table 2. *Effects of Stauprimide, DZNep, and their combination on the expression of cell cycle and apoptosis-related genes in the MCF-7 cell line.*

Genes	Stauprimide Fold change	p-value	DZNep Fold change	p-value	Combination Fold change	p-value
E2F1	-1.59	p = .000040	– 0.45	p = .002698	-3.64	p = .000009
CCNB1	– 1.25	p = .000040	– 0.05	p = .328024	-2.18	p = .000009
BAD	2.16	p = .000003	3.79	p < .000001	1.78	p = .000007
RB1	3.13	p = .000016	3.36	p = .000013	2.46	p = .000031
BCL2	3.33	p = .000019	2.18	p = .000059	3.74	p = .000014
CDKN1A	13.56	p = .000010	9.70	p = .000043	7.48	p = .000081

Quantitative real-time PCR (qRT-PCR) analysis was performed to assess changes in gene expression following treatment with Stauprimide, DZNep, or their combination at respective IC_{50} or ED_{50} concentrations for 72nd hours. Fold change values represent relative expression compared to untreated controls and were calculated using the $2^{-\Delta\Delta Ct}$ method. GAPDH and ACTB were used as reference genes. Significance was evaluated using Student's t-test (p < .05 was considered significant). Genes evaluated include markers related to cell cycle progression (E2F1, CCNB1), apoptosis regulation (BAD, BCL2), and tumor suppression (RB1, CDKN1A/p21). Fold change values >1 indicate upregulation; values <1 (negative) indicate downregulation relative to untreated control. Stauprimide = Stau; DZNep = DZN; p-value: probability value indicating significance. E2F1, E2F Transcription Factor 1; CCNB1, Cyclin B1; BAD, BCL2-Associated Agonist of Cell Death; RB1, Retinoblastoma 1; BCL2, B-cell Lymphoma 2; CDKN1A, Cyclin-Dependent Kinase Inhibitor 1A (p21)

Table 3. *Effects of Stauprimide, DZNep, and their combination on the expression of cell cycle regulatory genes in the MDA-MB-231 cell line.*

Genes	Stauprimide Fold change	p-value	DZNep Fold change	p-value	Combination Fold change	p-value
CDKN1A	-2.94	p = .000280	– 1.88	0.000641	-4.06	p = .000198
CDKN2A	2.36	p = .000012	3.73	0.000003	8.02	p < .000001

Quantitative real-time PCR was used to assess the transcriptional changes in cell cycle inhibitor genes CDKN1A (p21) and CDKN2A (p16) following treatment with Stauprimide, DZNep, or their combination for 72nd hours. Treatments were administered at concentrations corresponding to the IC_{50} or ED_{50} of each agent. Relative gene expression was calculated using the 2-ΔΔCt method, with GAPDH and ACTB as endogenous reference controls. CDKN1A, Cyclin-Dependent Kinase Inhibitor 1A (p21); CDKN2A, Cyclin-Dependent Kinase Inhibitor 2A (p16INK4a)

Table 4. *Effects of Stauprimide, DZNep, and their combination on gene expression profiles in the non-tumorigenic mammary epithelial cell line MCF-10A.*

Genes	Stauprimide Fold change	p-value	DZNep Fold change	p-value	Combination Fold change	p-value
E2F1	-10.41	p < .000001	-9.15	p < .000001	-14.47	p < .000001
CCNB1	-2.00	p = .000066	-1.55	p = .000119	-5.64	p = .000019
TP53	-0.10	p = .000027	-1.05	p < .000001	-2.06	p < .000001
APAF1	2.01	p = .000022	1.57	p = .000050	-1.59	p = .000091
CDKN1A	-1.43	p = .000718	-4.32	p = .000107	-1.51	p = .000586
BAD	2.94	p < .000001	0.17	p = .011262	-0.91	p = .000040
CDKN1B	3.10	p < .000001	-0.20	p = .012223	-0.81	p = .000084
BAX	2.98	p = .000002	0.66	p = .000007	-0.78	p = .000001
CDK2	3.26	p = .000045	2.62	p = .000075	-0.51	p = .014666
CDKN2A	3.09	p = .000067	2.38	p = .000079	-0.16	p = .097238
BCL2	3.92	p = .000010	2.21	p = .000048	1.54	p = .000144

Gene expression changes in MCF-10A cells were evaluated following 72-hour treatment with Stauprimide, DZNep, or their combination at IC_{50}/ED_{50} concentrations. Quantitative real-time PCR was performed to assess transcriptional modulation of key genes involved in cell cycle regulation, apoptosis, and DNA damage response. GAPDH and ACTB served as endogenous controls, and relative expression was calculated using the 2-ΔΔCt method. E2F1, E2F Transcription Factor 1; ; CCNB1, Cyclin B1; ; TP53, Tumor Protein p53; ; APAF1, Apoptotic Peptidase Activating Factor 1; ; CDKN1A, Cyclin-Dependent Kinase Inhibitor 1A (p21); ; BAD, BCL2-Associated Agonist of Cell Death; ; CDKN1B, Cyclin-Dependent Kinase Inhibitor 1B (p27Kip1); ; BAX, BCL2-Associated X Protein; ; CDK2, Cyclin-Dependent Kinase 2; ; CDKN2A, Cyclin-Dependent Kinase Inhibitor 2A (p16INK4a); ; BCL2, B-cell Lymphoma 2.

Table 5. *Effects of Stauprimide, DZNep, and their combination on the expression of regulatory genes in breast cancer stem cells (BCSCs).*

Genes	Stauprimide Fold change	p-value	DZNep Fold change	p-value	Combination Fold change	p-value
BAD	4.57	p < .000001	-1.59	p = .000013	-1.25	p = .000025
CCNB1	0.41	p = .004741	-1.28	p = .000121	2.88	p = .000004
TP53	-0.76	p = .007613	-1.28	p = .001494	4.45	p = .000050
E2F1	8.16	p < .000001	6.06	p = .000002	4.75	p = .000004
CDKN1B	-5.64	p = .000047	-0.53	p = .008307	5.50	p = .000005
CCND1	10.27	p = .000003	-2.84	p = .000217	12.69	p < .000001

Gene expression profiling was conducted in BCSC-enriched populations following 72-hour exposure to Stauprimide, DZNep, or their 1:1 combination at IC_{50} or ED_{50} concentrations. Quantitative real-time PCR (qRT-PCR) was used to quantify expression levels of key genes involved in apoptosis, cell cycle progression, and transcriptional regulation. Data were normalized to GAPDH and ACTB reference genes, and relative fold changes were calculated using the $2^{-\Delta\Delta Ct}$ method. Fold change values indicate upregulation (>1) or downregulation (<1, negative values) compared to untreated controls. Statistical significance was determined using Student's t-test (p < .05). Notably, combination treatment led to a marked upregulation of tumor suppressor gene TP53 (4.45-fold, p < .001) and cell cycle inhibitor CDKN1B (5.50-fold, p < .001), while also restoring CCND1 expression suppressed by DZNep alone. These findings suggest that the combination may counterbalance single-agent gene modulation and enhance regulatory control over stem-like breast cancer cells. TP53, tumor protein p53; BAD, BCL2-associated agonist of cell death; E2F1, E2F transcription factor 1; CDKN1B, cyclin-dependent kinase inhibitor 1B; CCNB1, cyclin B1; CCND1, cyclin D1.

4. DISCUSSION

Breast cancer presents significant challenges for effective treatment due to its heterogeneous nature and therapy-resistant subpopulations. In this context, combining epigenetic modulators and differentiation-inducing agents has been proposed as a promising strategy, potentially delivering more selective and potent anti-cancer effects compared to conventional therapies alone [30]. In the present study, we comprehensively evaluated the cytotoxic, apoptotic, anti-proliferative, and molecular impacts of combining the epigenetic inhibitor 3-Deazaneplanocin A (DZNep) with the differentiation-promoting agent Stauprimide on various breast cancer cell lines.

Initially, our findings demonstrated that a 1:1 combination of DZNep and Stauprimide exhibited synergistic cytotoxicity against MCF-7 and MDA-MB-231 breast cancer cell lines, with combination index (CI) values of 0.671 and 0.134, respectively. According to the Chou-Talalay methodology, these CI values represent strong synergistic interactions [28]. Notably, combination therapy significantly reduced the required therapeutic dose of DZNep by approximately 84 – to 502-fold, as indicated by dose-reduction index (DRI) analyses. Such substantial dose reductions highlight the potential for minimizing treatment-related systemic toxicity.

Previous studies have reported varying IC_{50} values for DZNep, including 5 µM at 72 hours in MCF-7 cells [31] and as low as 235 nM at 144 hours in MDA-MB-231 cells [32]. However, these variations may be attributed to differences in cell culture conditions, cell densities, and experimental methods employed. Our study observed higher IC_{50} values for DZNep, yet demonstrated that these therapeutic doses could be significantly lowered through combination strategies, emphasizing the clinical relevance of drug combinations to enhance efficacy and reduce potential adverse effects.

Apoptosis analyses further revealed that treatment with DZNep and Stauprimide, both individually and in combination, significantly induced apoptosis in MCF-7 and breast cancer stem cell (BCSC) populations, while apoptosis levels in normal mammary epithelial MCF-10A cells remained comparatively lower. These findings align with previous literature highlighting DZNep's selective pro-apoptotic effects in cancer cells [31]. Additionally, De La Rosa et al. previously demonstrated synergistic apoptotic effects of DZNep combined with Panobinostat and Temozolomide in glioblastoma models [33], further validating the potential therapeutic utility of combination therapies involving epigenetic agents.

Cell cycle analysis indicated that Stauprimide primarily induced G2/M phase arrest in breast cancer cells, notably causing a substantial increase (4.11-fold relative to untreated control) in the MCF-7 cell line, accompanied by significant polyploidy. This observation is consistent with previous reports by Gallala et al., which demonstrated similar G2/M arrest and polyploidy induction by Stauprimide in small-cell lung carcinoma cells [34]. It is hypothesized that this cell cycle arrest is linked to defective cytokinesis and subsequent induction of apoptosis.

The effects of DZNep on cell cycle progression have been reported to vary based on the cancer cell type, including G1/S arrest in glioblastoma [35] and G1 phase accumulation in lung cancer models [36]. In our study, DZNep treatment prominently induced G0/G1 arrest in MCF-7 cells (70.8%), whereas the effect on MDA-MB-231 cells was limited to moderate G2/M arrest. Interestingly, combination therapy resulted in cell-type-specific effects, including pronounced G2/M arrest and moderate polyploidy in MCF-7 cells, and increased G0/G1 phase arrest in MDA-MB-231 cells. These differential responses highlight the complexity and specificity of cell cycle modulation by combination therapies.

Migration assays demonstrated that treatment with Stauprimide and DZNep, both individually and in combination, significantly inhibited migration in MCF-7, MDA-MB-231, and BCSC cells. This finding supports previous observations by Girard et al., which demonstrated reduced migration following DZNep treatment in chondrosarcoma cells [37], as well as studies by Hibino et al., indicating similar anti-migratory effects of DZNep in gastric (AGS) and laryngeal (Hep-2) cancer cells [38]. Although the combination treatment also impacted migration in normal MCF-10A cells, the magnitude of this effect was notably less pronounced than that observed in cancer cells, further underscoring the selective anti-metastatic potential of this therapeutic combination.

Gene expression analysis demonstrated significant upregulation of key tumor suppressor genes (e.g., RB1, p21, p27) following DZNep treatment, consistent with previously reported effects in AML-3 leukemia and breast cancer cell lines [19, 20, 31]. Furthermore, Stauprimide treatment notably increased expression of RB1 and p21 in MCF-7 cells and p16 in MDA-MB-231 cells. The combination therapy significantly upregulated TP53 and p27 gene expression in the BCSC population, highlighting the potential of this combination to suppress tumor-initiating capabilities inherent to cancer stem cells. Activation of TP53, a well-established tumor suppressor gene, has been previously linked to enhanced differentiation and suppression of cancer stem cell phenotypes [39].

Collectively, our data indicate that both DZNep and Stauprimide, alone and especially in synergistic combination, demonstrate therapeutic potential in breast cancer through induction of cell cycle arrest, apoptosis, inhibition of migration, and modulation of tumor suppressor gene expression. The pronounced effects observed on cancer stem cells provide additional translational relevance, offering promising avenues to prevent tumor recurrence and metastasis, thereby highlighting the clinical potential of this combination regimen.

5. CONCLUSION

In the present study, we comprehensively evaluated the anticancer potential of combining the epigenetic methyltransferase inhibitor DZNep with the MYC transcription inhibitor Stauprimide in multiple breast cancer cell lines. Our findings revealed that a 1:1 combination of these agents exhibited robust synergistic cytotoxicity, particularly in MCF-7 (luminal A) and MDA-MB-231 (triple-negative) breast cancer cells. This combined treatment effectively induced apoptosis, promoted cell cycle arrest accompanied by polyploidy, and significantly inhibited cell migration, even at substantially reduced concentrations. Notably, gene expression changes observed in breast cancer stem cells (BCSCs), such as significant upregulation of tumor suppressor genes *TP53* and p27, highlight the combination's potential for preventing recurrence and metastasis. Furthermore, the limited cytotoxicity and apoptosis detected in the non-tumorigenic mammary epithelial cell line MCF-10A emphasize the selective antitumor profile of this therapeutic combination, thereby suggesting a lower risk of systemic toxicity, which is clinically advantageous.

In conclusion, the combination of DZNep and Stauprimide represents a promising therapeutic strategy against breast cancer, demonstrating potent anticancer effects through the induction of apoptosis, inhibition of migration, and modulation of tumor suppressor gene expression across diverse cellular subtypes. This approach holds potential for overcoming epigenetic drug resistance mechanisms and specifically targeting cancer stem cells, either as an adjunct or alternative to current chemotherapeutic modalities. Further validation of these findings using in vivo tumor models and preclinical animal studies will be an essential next step toward clinical translation and integration into future breast cancer treatment protocols.

Funding: *The author(s) received no financial support for the research.*

Conflicts of interest: *The authors declare that they have no conflict of interest.*

Peer-review: *Externally peer-reviewed.*

Author Contributions:

Research idea: CC, TBO, CG

Design of the study: CC, TBO, CG

Acquisition of data for the study: CC, CK, BOY, AA, RG, ET

Analysis of data for the study: CC, CK, CG

Interpretation of data for the study: CC, CK, CG

Drafting the manuscript: CC, TBO, CG

Revising it critically for important intellectual content: CC, TBO, CK, BOY, AA, RG, ET

Final approval of the version to be published: CC, TBO, CK, BOY, AA, RG, ET

REFERENCES

[1] Sung H, Ferlay J, Siegel RL, Laversanne M, Soerjomataram I, Jemal A, Bray F. Global cancer statistics 2020: globocan estimates of incidence and mortality worldwide for 36 cancers in 185 countries. CA Cancer J Clin. 2021;71(3):209–249. https://doi.org/10.3322/CAAC.21660

[2] World Health Organization.Global Breast Cancer Initiative Implementation Framework. Published [2023]. https://iris.who.int/bitstream/handle/10665/365784/978.924.0067134-eng.pdf

[3] Rakha EA, Reis-Filho JS, Ellis IO. Basal-like breast cancer: A critical review. J Clin Oncol. 2008; 20;26(15):2568-2581. https://doi.org/10.1200/JCO.2007.13.1748

[4] Perou CM, Sørile T, Eisen MB, Van De Rijn M, Jeffrey SS, Ress CA, Pollack J R, Ross D T, Johnsen H, Akslen L A, Fluge O, Pergamenschikov A, Williams C, Zhu S X, Lønning P E, Børresen-Dale A L, Brown P O, Botstein D. Molecular portraits of human breast tumours. Nature. 2000; 406(6797):747-752. https://doi.org/10.1038/35021093

[5] Ginestier C, Hur MH, Charafe-Jauffret E, Monville F, Dutcher J, Brown M, Jacquemier J, Viens P, Kleer CG, Liu S, Schott A, Hayes D, Birnbaum D, S Wicha M, Dontu G. ALDH1 is a marker of normal and malignant human mammary stem cells and a predictor of poor clinical outcome. Cell Stem Cell. 2007;1(5):555-567. https://doi.org/10.1016/j.stem.2007.08.014

[6] Al-Hajj M, Wicha MS, Benito-Hernandez A, Morrison SJ, Clarke MF. Prospective identification of tumorigenic breast cancer cells. Proc Natl Acad Sci U S A. 2003;100(7):3983-3988. https://doi.org/10.1073/pnas.053.029.1100

[7] Visvader JE, Lindeman GJ. Cancer stem cells: Current status and evolving complexities. Cell Stem Cell. 2012;10(6):717-728. https://doi.org/10.1016/j.stem.2012.05.007

[8] Dontu G, Al-Hajj M, Abdallah WM, Clarke MF, Wicha MS. Stem cells in normal breast development and breast cancer. Cell Prolif. 2003;36 (Suppl 1):59-72. https://doi.org/10.1046/J.1365-2184.36.S.1.6.X

[9] Reya T, Morrison SJ, Clarke MF, Weissman IL. Stem cells, cancer, and cancer stem cells. Nature. 2001;414(6859):105-111. https://doi.org/10.1038/35102167

[10] Ferrari P, Scatena C, Ghilli M, Bargagna I, Lorenzini G, Nicolini A. Molecular mechanisms, biomarkers and emerging therapies for chemotherapy resistant TNBC. Int J Mol Sci. 2022;23(3):1665. https://doi.org/10.3390/ijms23031665

[11] Dean M, Fojo T, Bates S. Tumour stem cells and drug resistance. Nat Rev Cancer. 2005;5(4):275-284. https://doi.org/10.1038/NRC1590

[12] Takebe N, Miele L, Harris PJ, Jeong W, Bando H, Kahn M, X Yang S, Ivy S P. Targeting Notch, Hedgehog, and Wnt pathways in cancer stem cells: clinical update. Nat Rev Clin Oncol.2015;12(8):445-464. https://doi.org/10.1038/nrclinonc.2015.61

[13] Patel SA, Ndabahaliye A, Lim PK, Milton R, Rameshwar P. Challenges in the development of future treatments for breast cancer stem cells. Breast Cancer (Dove Med Press). 2010; 2:1-11. PMCID: PMC3004231

[14] Makena MR, Ranjan A, Thirumala V, Reddy AP. Cancer stem cells: Road to therapeutic resistance and strategies to overcome resistance. Biochimica et Biophysica Acta (BBA) – Molecular Basis of Disease 2020; 1;1866(4):165339. https://doi.org/10.1016/j.bbadis.2018.11.015

[15] Wu HJ, Chu PY. Epigenetic regulation of breast cancer stem cells contributing to carcinogenesis and therapeutic implications. Int J Mol Sci. 2021;22(15):8113. https://doi.org/10.3390/IJMS22158113

[16] Verona F, Pantina V D, Modica C, Lo Iacono M, D'Accardo C, Porcelli G, Cricchio D, Turdo A, Gaggianesi M, Di Franco S, Todaro M, Veschi V, Stassi G. Targeting epigenetic alterations in

cancer stem cells. Front Mol Med. 2022; 2:1011882. https://doi.org/10.3389/FMMED.2022.101.1882

[17] Suraweera A, O'Byrne KJ, Richard DJ. Epigenetic drugs in cancer therapy. Cancer Metastasis Rev. 2025;44:37. https://doi.org/10.1007/S10555.025.10253-7

[18] Gonzalez ME, DuPrie ML, Krueger H, Merajver SD, Ventura AC, Toy KA, Kleer CG. Histone methyltransferase EZH2 induces Akt-dependent genomic instability and BRCA1 inhibition in breast cancer. Cancer Res. 2011; 71 (6): 2360–2370. https://doi.org/10.1158/0008-5472.CAN-10-1933

[19] Sun F, Chan E, Wu Z, Yang X, Marquez VE, Yu Q. Combinatorial pharmacologic approaches target EZH2-mediated gene repression in breast cancer cells. Mol Cancer Ther. 2009; 8(12):3191-3202 https://doi.org/10.1158/1535-7163.mct-09-0479

[20] Fiskus W, Wang Y, Sreekumar A, Buckley KM, Shi H, Jillella A, Ustun C, Rao R, Fernandez P,Chen J, Balusu R, Koul S, Atadja P, Marquez V E,Bhalla K N. Combined epigenetic therapy with the histone methyltransferase EZH2 inhibitor 3-deazaneplanocin A and the histone deacetylase inhibitor panobinostat against human AML cells. Blood 2009; 114 (13): 2733–2743.https://doi.org/10.1182/blood-2009-03-213496

[21] Yu J, Liu D, Yuan Y, Sun C, Su Z. Rethinking MYC inhibition: A multi-dimensional approach to overcome cancer's master regulator. Front Cell Dev Biol. 2025;13:1601975. https://doi.org/10.3389/fcell.2025.160.1975

[22] Duan Y, Liu Z, Wang Q, Zhang J, Liu J, Zhang Z, Li C. Targeting MYC: Multidimensional regulation and therapeutic strategies in oncology. Genes & Diseases. 2025;12(4):101435. https://doi.org/10.1016/j.gendis.2024.101435

[23] Bouvard C, Lim SM, Ludka J, Yazdani N, Woods AK, Chatterjee AK, Schultz P G, Shoutian Z. Small molecule selectively suppresses MYC transcription in cancer cells. Proc Natl Acad Sci U S A. 2017;114(13):3497-3502. https://doi.org/10.1073/pnas.170.266.3114

[24] Jha RK, Kouzine F, Levens D. MYC function and regulation in physiological perspective. Front Cell Dev Biol. 2023;11:1268275. https://doi.org/10.3389/fcell.2023.126.8275

[25] Tahamtani Y, Azarnia M, Farrokhi A, Moradmand A, Mirshahvaladi S, Aghdami N, Baharvand H. Stauprimide priming of human embryonic stem cells toward definitive endoderm. Cell J. 2014; 16(1):63-72.

[26] Antonsson Andreas, Persson L J. Induction of apoptosis by staurosporine involves the inhibition of expression of the major cell cycle proteins at the $G_{(2)}$/M checkpoint accompanied by alterations in Erk and Akt kinase activities. Anticancer Res. 2009; 29(8):2893 – 2898.

[27] Liu Y, Yang Q. The roles of EZH2 in cancer and its inhibitors. Med Oncol. 2023; 40(6):167 https://doi.org/10.1007/S12032.023.02025-6

[28] Chou TC. Theoretical basis, experimental design, and computerized simulation of synergism and antagonism in drug combination studies. Pharmacol Rev. 2006; 58(3):621-681. https://doi.org/10.1124/PR.58.3.10

[29] Livak KJ, Schmittgen TD. Analysis of relative gene expression data using real-time quantitative PCR and the $2^{-\Delta\Delta CT}$ Method. Methods 2001;25:402–408. https://doi.org/10.1006/meth.2001.1262

[30] Kang Z, Wang J, Liu J, Du L, Liu X. Epigenetic modifications in breast cancer: from immune escape mechanisms to therapeutic target discovery. Front Immunol. 2025;16:1584087. https://doi.org/10.3389/fimmu.2025.158.4087

[31] Tan J, Yang X, Zhuang L, Jiang X, Chen W, Puay LL, Karuturi RKM, Boon Ooi Tan P, Liu T E, Yu Q. Pharmacologic disruption of Polycomb-repressive complex 2-mediated gene repression selectively induces apoptosis in cancer cells. Genes Dev. 2007; 21(9):1050-1063. https://doi.org/10.1101/GAD.1524107

[32] Hayden A, Johnson PWM, Packham G, Crabb SJ. S-adenosylhomocysteine hydrolase inhibition by 3-deazaneplanocin A analogues induces anti-cancer effects in breast cancer cell lines and synergy with both histone deacetylase and HER2 inhibition. Breast Cancer Res Treat. 2011; 127(1):109-119. DOI: 10.1007/s10549.010.0982-0

[33] De La Rosa J, Urdiciain A, Zazpe I, Zelaya M V., Meléndez B, Rey JA, Idoate M A, Castresana J S. The synergistic effect of DZNEP, panobinostat and temozolomide reduces clonogenicity and induces apoptosis in glioblastoma cells. Int J Oncol. 2020; 56(1):283-300. https://doi.org/10.3892/IJO.2019.4905

[34] Gallala H, Winter J, Veit N, Nowak M, Perner S, Courts C, Kraus D, Janzen V, Probstmeier R. Staurosporine analogs promote distinct patterns of process outgrowth and polyploidy in small cell lung carcinoma cells. Tumor Biology. 2015; 36 (4):2725-2735. DOI: 10.1007/s13277.014.2897-6

[35] Kikuchi J, Takashina T, Kinoshita I, Kikuchi E, Shimizu Y, Sakakibara-Konishi J, Oizumi S, Marquez V E, Nishimura M, Dosaka-Akita H. Epigenetic therapy with 3-deazaneplanocin A, an inhibitor of the histone methyltransferase EZH2, inhibits growth of non-small cell lung cancer cells. Lung Cancer. 2012 ;78(2):138-143. https://doi.org/10.1016/j.lungcan.2012.08.003

[36] Zhang K, Sun X, Zhou X, Han L, Chen L, Shi Z, Zhang A, Ye M, Wang Q, Liu C, Wei J, Ren Y, Yang J, Zhang J, Pu P, Li M, Kang C. Long non-coding RNA HOTAIR promotes glioblastoma cell cycle progression in an EZH2 dependent manner. Oncotarget 2015; 6(1):537-546. https://doi.org/10.18632/oncotarget.2681

[37] Girard N, Bazille C, Lhuissier E, Benateau H, Llombart-Bosch A, Boumediene K, Bauge C. 3-Deazaneplanocin A (DZNep), an inhibitor of the histone methyltransferase EZH2, induces apoptosis and reduces cell migration in chondrosarcoma cells. PLoS One 2014; 9(5):e98176. https://doi.org/10.1371/journal.pone.0098176

[38] Hibino S, Saito Y, Muramatsu T, Otani A, Kasai Y, Kimura M, Saito H. Inhibitors of enhancer of zeste homolog 2 (EZH2) activate tumor-suppressor microRNAs in human cancer cells. Oncogenesis 2014; 3(5):e104. https://doi.org/10.1038/oncsis.2014.17

[39] Pitolli C, Wang Y, Mancini M, Shi Y, Melino G, Amelio I. Do mutations turn p53 into an oncogene? Int J Mol Sci. 2019; 20(24):6241.https://doi.org/10.3390/IJMS20246241